From SEFES to SEAMES: change across three decades in phytoplankton pigment composition

Jackson Griffin

650059

KAA309 Research Project

3,060 words

Abstract

This study compares phytoplankton community structure across three decades on the southeast Australian shelf using pigment and hydrographic data from the South East Fishery Ecosystem Surveys (1996) and South East Australian Marine Ecosystem Surveys (2023–2025). Pigments quantified by HPLC served as functional markers for phytoplankton groups, and multivariate analyses (NMDS, dbRDA) related pigment variability to temperature, mixed-layer depth (MLD), and nitrate. Diatoms remained regionally important, but recent assemblages were characterised by higher nitrate, deeper MLDs, and stronger stratification under an intensified East Australian Current (EAC). Communities showed increased prasinophyte and chlorophyte representation, indicating a shift toward smaller, faster-growing taxa adapted to warm, nutrient-variable conditions, although episodic eddies and upwelling still supported transient diatom blooms. The results highlight a transition toward nano- and picoplankton dominance, driven by changing physical-biogeochemical coupling, with implications for productivity, trophic transfer, and carbon export in a rapidly warming boundary-current system.

Introduction

Marine ecosystems are dynamic systems whose structure and productivity are shaped by interactions among circulation, nutrient supply, and biological processes. Along the southeastern Australian shelf and Bass Strait, ecological change has accelerated in recent decades due to climate forcing and sustained fishing pressure (Bax & Williams, 2000; Ridgway & Ling, 2023). Documented alterations span trophic levels—from phytoplankton and zooplankton communities to benthic habitats and fish assemblages (Poloczanska et al., 2013). Understanding the mechanisms driving these transformations is essential for predicting ecosystem trajectories and guiding adaptive management.

Prompted by declining commercial fish stocks (Edgar et al., 2018), the South-East Australian Marine Ecosystem Survey (SEAMES), coordinated by CSIRO, investigates the causes of these declines. Three integrative hypotheses frame this research: the Habitat Hypothesis (fishing impacts on benthic environments), the Climate Hypothesis (effects of ocean warming and stratification), and the Trophic Hypothesis (combined fishing and climate effects on food-web structure). This study addresses the Trophic Hypothesis by examining how changes in oceanographic conditions—particularly those linked to the East Australian Current (EAC)—influence phytoplankton community structure, pigment composition, and trophic pathways.

Phytoplankton form the energetic foundation of marine ecosystems, linking nutrient dynamics to higher trophic levels (Falkowski, 2012; Behrenfeld & Boss, 2006). Their composition and size structure respond rapidly to light, temperature, and nutrient availability (Winder & Sommer, 2012). In temperate systems such as southeastern Australia, these drivers are strongly modulated by the EAC—a warm, nutrient-poor

boundary current whose intensification has enhanced stratification, surface warming, and eddy activity (Everett et al., 2012). Mixed-layer depth (MLD) regulates phytoplankton growth by controlling light exposure and nutrient fluxes to the euphotic zone (Brewin et al., 2015). Eddies, fronts, and wind-driven mixing events can locally deepen the MLD, entraining nutrients and supporting transient diatom blooms amid otherwise oligotrophic conditions (Zhou et al., 2025). Conversely, shallow mixed layers restrict nutrient replenishment, favouring smaller, low-nutrient-adapted taxa.

High-performance liquid chromatography (HPLC) enables quantitative assessment of such community shifts using diagnostic pigments as taxonomic and functional markers. Key pigment–phytoplankton associations used here (Table 1) include fucoxanthin (diatoms), peridinin (dinoflagellates), alloxanthin (cryptophytes), prasinoxanthin (prasinophytes), 19'-hexanoyloxyfucoxanthin (haptophytes), and 19'-butanoyloxyfucoxanthin (pelagophytes). These pigments act as proxies for functional groups, allowing reconstruction of community composition under varying hydrographic conditions (Jeffrey, 1974; Uitz et al., 2006).

Table 1 – Pigment-phytoplankton associations.

Pigment	Phytoplankton type				
Fucoxanthin	Abundant in diatoms, also observed in haptophytes,				
	dinoflagellates, Chrysophytes, pelagophytes, raphidophytes				
Peridinin	Dinoflagellates- type 1				
Alloxanthin	Cryptophytes				
Prasinoxanthin	Prasinophytes				
DVChl a, DVChl b	Prochlorophytes				
Zeaxanthin	Widespread but marker in Cyanobacteria				
Chlorophyll b	Chlorophytes, Prasinophytes				
Lutein	Chlorophytes, Prasinophytes				
Neoxanthin, violaxanthin	Green algae (Chlorophytes, prasinophytes)				
19-Hex Fucoxanthin	Haptophytes, some dinoflagellates				
19- But Fucoxanthin	Pelagophytes , haptophytes				
Chl C1, Chl C2, Chl C3	Widespread				
Diadinoxanthin, diatoxanthin	widespread				

By comparing pigment and hydrographic data from historical South-East Fishery Ecosystem Surveys (SEFES, 3 voyages, 1990s) and recent SEAMES voyages (4 voyages, 2020s), this study evaluates how phytoplankton communities have responded to evolving physical and biogeochemical conditions over three decades. Specifically, it tests how variations in temperature, MLD, and nutrient availability influence pigment composition and inferred size structure. The overarching aim is to identify long-term and environmental drivers of phytoplankton community change and assess implications for productivity, trophic transfer, and carbon export in a rapidly changing boundary-current system.

Methods

Data sources and sampling

This study integrated historical data from the South East Fishery Ecosystem Surveys (SEFES, 1996) and contemporary data from the South East Australian Marine Ecosystem Surveys (SEAMES, 2023–2025) to assess long-term changes in phytoplankton pigment composition and environmental drivers across the southeast Australian shelf. SEFES samples were collected aboard the RV Southern Surveyor, and SEAMES samples aboard the RV Investigator (Fig. 1, Table 2).

At each SEAMES station, a 36-bottle conductivity–temperature–depth (CTD) rosette equipped with 12 L Niskin bottles collected water from multiple depths within the euphotic zone. Sampling was conducted opportunistically each morning and aligned with trawl locations, rather than being specifically designed for the purpose of this study. Temperature, salinity, oxygen, and nutrient concentrations (nitrate + nitrite = NOx) were measured in situ or from subsamples. Pigment samples were taken from the surface and the deep chlorophyll maximum (DCM), as indicated by the fluorescence trace on the downward CTD profile. These were filtered from known water volumes onto GF/F filters and stored at $-80\,^{\circ}$ C until analysis. Comparable sampling and analytical procedures were followed during SEFES (Bax & Williams, 2000).

Pigment analysis

Chlorophyll and accessory pigments were quantified via high-performance liquid chromatography (HPLC) following CSIRO oceanographic protocols (Hooker et al., 2012). Individual pigments were identified and calibrated against reference standards, with results expressed in mg ${\rm m}^{-3}$. Diagnostic pigments were assigned to major phytoplankton functional types (Table 1).

Data treatment and statistical analysis

All data processing and visualisation were performed in R v4.4.3 using the packages *tidyverse*, *vegan*, *ggordiplots*, and *ggplot2*. Pigment concentrations were square-root transformed to downweight dominant pigments such as chlorophyll a and stabilise variance among samples; more severe transformations, including $\log(x+1)$, were tested but did not improve statistical performance. For SEFES, pigment data was aligned with its corresponding CTD and nutrient profiles based on location and time, ensuring comparability across hydrographic and biogeochemical variables.

Phytoplankton community structure was examined using non-metric multidimensional scaling (NMDS) based on Bray–Curtis dissimilarity, suitable for ecological abundance

data. Environmental variables (temperature, MLD, and nitrate) were fitted onto NMDS ordinations with the *envfit* function to visualise significant gradients.

To quantify pigment–environment relationships, distance-based redundancy analyses (dbRDA) were run separately for SEFES and SEAMES using *capscale* and *adonis2* in *vegan*. Bray–Curtis dissimilarities of square-root-transformed pigment data formed the response matrix. Analysing datasets separately enabled evaluation of whether pigment–environment associations were consistent through time or had shifted under different hydrographic regimes. Predictor significance and model fit were assessed via 999-permutation tests, and adjusted R² values quantified explained variance.

Comparative framework

Mean voyage-level hydrographic parameters (SST, MLD, DCM, nitrate) were calculated to contextualise pigment variation (Table 2). Other variables (salinity, phosphate, silicate) were also tested but were strongly collinear with the retained predictors and therefore excluded from multivariate models. Cross-decadal comparisons focused on differences in pigment composition, total pigment biomass, and environmental coupling between SEFES and SEAMES voyages. Combined NMDS and dbRDA analyses provided an integrated view of how phytoplankton functional composition and inferred size structure respond to evolving physical drivers within an increasingly dynamic East Australian Current system.

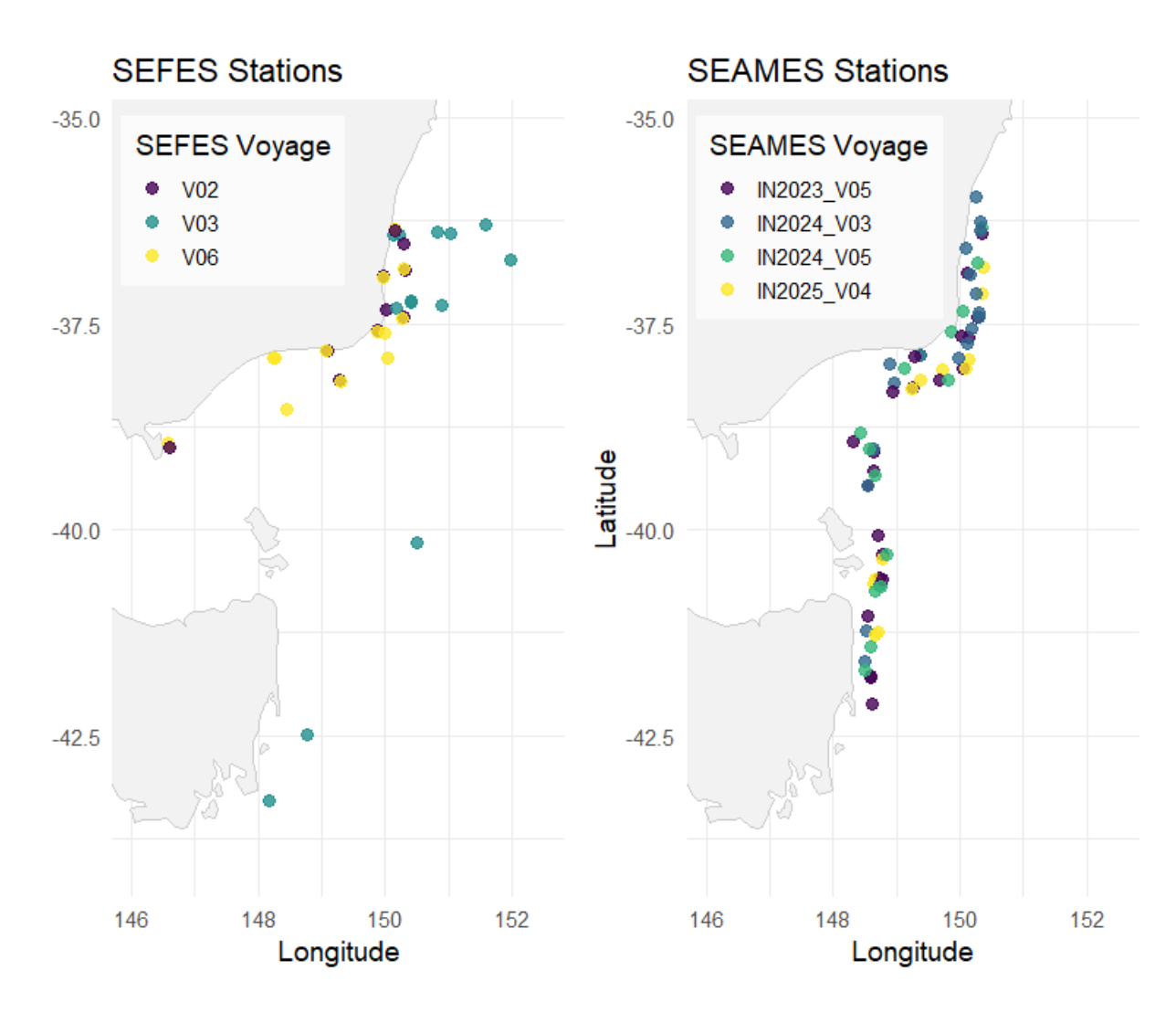


Figure 1 – Map of SEFES and SEAMES sampling stations.

Results

Oceanographic conditions across voyages

Hydrographic conditions varied markedly between voyages and across decades, reflecting the interplay between temperature, stratification, and nutrient supply (Table 2; Fig. 2). Surface temperatures at ~5m depth ranged from 14.3–21.2°C during the SEFES cruises of 1996 and from 13.9–21.3°C during the SEAMES voyages of the 2020s. The warmest conditions were observed during SEFES SS1996 V03 (May 1996) and SEAMES IN2024_V03 (May 2024), while cooler conditions characterised SEFES SS1996 V06 (November–December 1996) and SEAMES IN2023_V05 (June–July 2023). These seasonal differences in surface heating were closely linked to variations in mixed layer depth and nutrient availability.

MLD reflected the balance between surface warming and wind-driven mixing. Conditions during IN2025_V04 produced the deepest MLDs (114.8 \pm 87.7 m),

consistent with enhanced vertical mixing. Across both datasets, the deep chlorophyll maximum (DCM) consistently occurred above the MLD, typically between 24–35 m, indicating that phytoplankton biomass was likely concentrated near the nutricline where light and nutrients co-occurred. Statistical analyses showed no significant differences in pigment composition between surface and DCM samples, so data from both depths were pooled for subsequent analyses.

Table 2 – Key voyage data. Sea surface temperature (°C) shown with min-max and mean ± standard deviation. MLD, deep chlorophyll maximum and nitrate all shown as mean ± standard deviation.

GROUP	VOYAGE	DATES	SST (°C)	MLD (m)	DCM (m)	Nitrate (µmol)
SEFES	SS199602	16/04-	15.8-20.9	55.7 ± 32.8	24.3 ± 9.5	1.03 ± 0.82
		12/05/1996	(17.3 ± 1.5)			
SEFES	SS199603	13/05-	14.3-21.2	50.1 ± 25.5	27.2 ± 18.3	1.96 ± 1.97
		27/05/1996	(18.3 ± 2)			
SEFES	SS199606	20/11-	14.4-16.5	32.8 ± 13.4	29.0 ± 17.7	0.71 ± 1.12
		19/12/1996	(15.4 ± 0.6)			
SEAMES	IN2023_V05	28/06-	13.9-17.5	96.6 ± 55.3	35.3 ± 19.3	3.29 ± 1.03
		30/07/2023	(15.6 ± 0.9)			
SEAMES	IN2024_V03	01/05-	16.1-21.3	67.1 ± 32.3	33.1 ± 27.5	1.26 ± 1.31
		31/05/2024	(18.7 ± 1.4)			
SEAMES	IN2024_V05	13/11-	13.9-20.4	52.6 ± 40.8	24.8 ± 14.1	1.21 ± 1.53
		12/12/2024	(17.1 ± 1.7)			
SEAMES	IN2025_V04	29/04-	14.7-19.6	114.8 ± 87.7	32.6 ± 38.4	2.31 ± 0.67
		18/05/2025	(16.9 ± 1.1)			

Nitrate distributions mirrored these physical patterns. Shallow, well-stratified conditions coincided with low surface nitrate, as in SS1996 V06 and IN2024_V05, where limited vertical exchange restricted nutrient resupply. Conversely, deeper mixed layers were associated with elevated nitrate, as during IN2023_V05 (3.29 \pm 1.03 μ mol L^{-1}) and IN2025_V04 (2.31 \pm 0.67 μ mol L^{-1}). The voyage SS1996 V03 was a notable outlier, combining relatively warm surface waters (18.3 \pm 2.0°C) with high and variable nitrate concentrations (1.96 \pm 1.97 μ mol L^{-1}), indicating episodic nutrient injection despite seasonal stratification. This coupling of warm SSTs with elevated nitrate highlights the dynamic nature of shelf–slope exchange processes in the region.

Conditions were variable within voyages, revealing several skewed distributions (Fig. 2). Nitrate concentrations during IN2023_V05 were generally high but exhibited a long negative tail, while IN2025_V04 showed a narrower, right-skewed distribution with a higher median. Similarly, SS1996 V03 displayed an uneven spread of nitrate values compared to the more depleted and less variable conditions in SS1996 V02 and SS1996 V06. These patterns demonstrate that temperature, stratification, and nutrient supply are tightly coupled: seasonal heating and mixing control MLD, which in turn regulates nutrient availability and the vertical structure of phytoplankton biomass. Each voyage

therefore represents a distinct ecological state shaped by the interaction of physical and biogeochemical drivers.

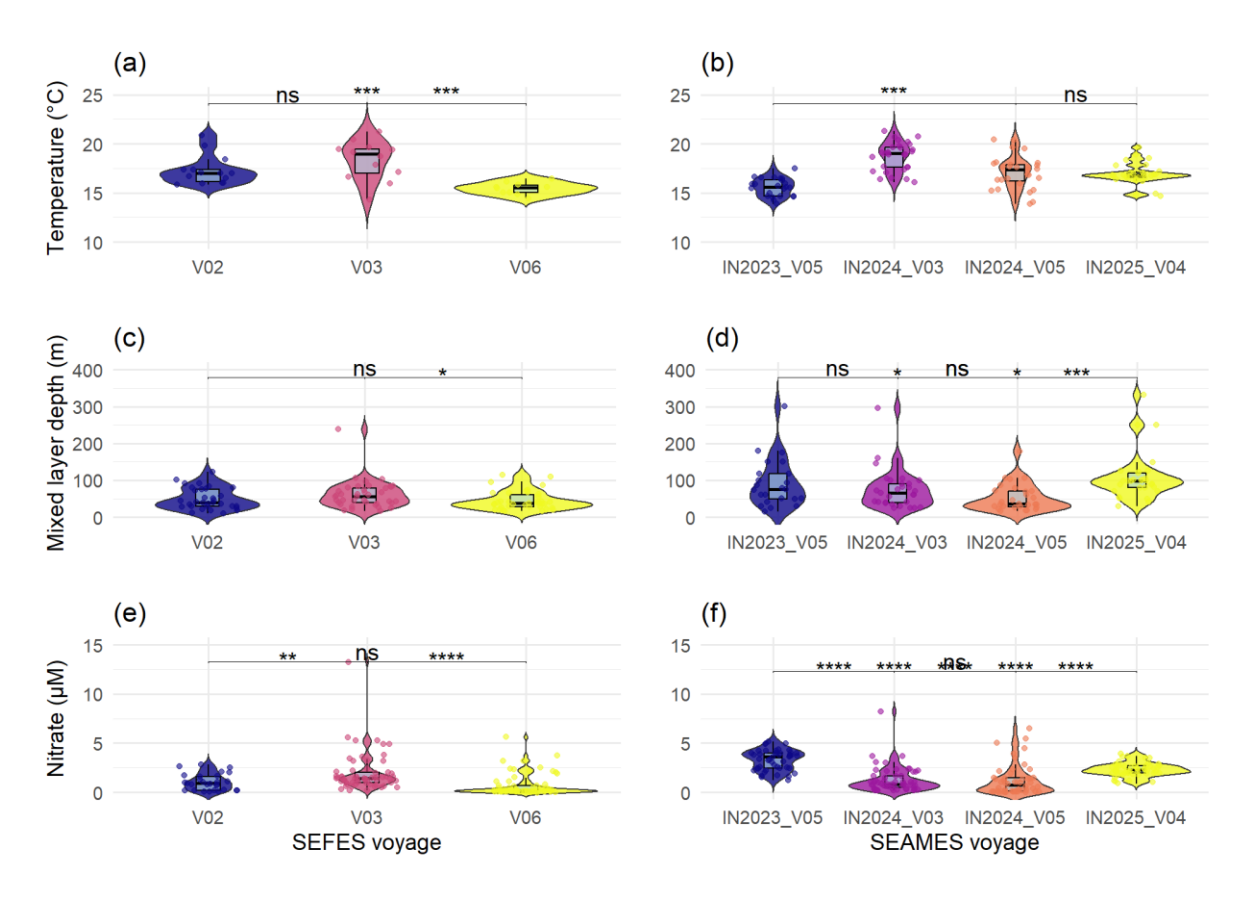


Figure 2 – Violin plots of surface temperature (~5 m; a–b), MLD (c–d) and nitrate (μ M; e-f) across SEFES and SEAMES voyages. Boxplots show medians and interquartile ranges. Significance levels are indicated as ns, * p < 0.05, **** p < 0.001.

Pigment composition and seasonal patterns

Pigment composition differed significantly between SEFES (1990s) and SEAMES (2020s), reflecting shifts in phytoplankton community structure and biomass (Fig. 3; Table S1). Overall, pigment concentrations were higher in SEAMES, with most diagnostic pigments showing significant positive differences relative to SEFES. Notably, violaxanthin, neoxanthin, prasinoxanthin, total chlorophyll b, 19'-butanoyloxyfucoxanthin, chlorophyll c_3 , peridinin, and degradation products such as phaeophytin a were all markedly higher in SEAMES (p < 0.001). These pigments are characteristic of prasinophytes, green algae, pelagophytes, and dinoflagellates—taxa that generally thrive under warm, stratified, and low-nutrient conditions—indicating increased representation of these groups in the recent dataset.

Fucoxanthin and alloxanthin were also elevated in SEAMES (p < 0.05), consistent with greater contributions from diatoms and cryptophytes under conditions favourable for

nutrient resupply. Conversely, zeaxanthin and diatoxanthin were significantly higher in SEFES, indicating a stronger presence of cyanobacteria, typically associated with warmer, variable-nutrient environments.

Total chlorophyll *a* concentrations were significantly greater in SEAMES (p < 0.01), confirming higher overall pigment biomass in the recent samples. These results collectively indicate that SEAMES conditions supported a more diverse and pigment-rich phytoplankton community than during SEFES.

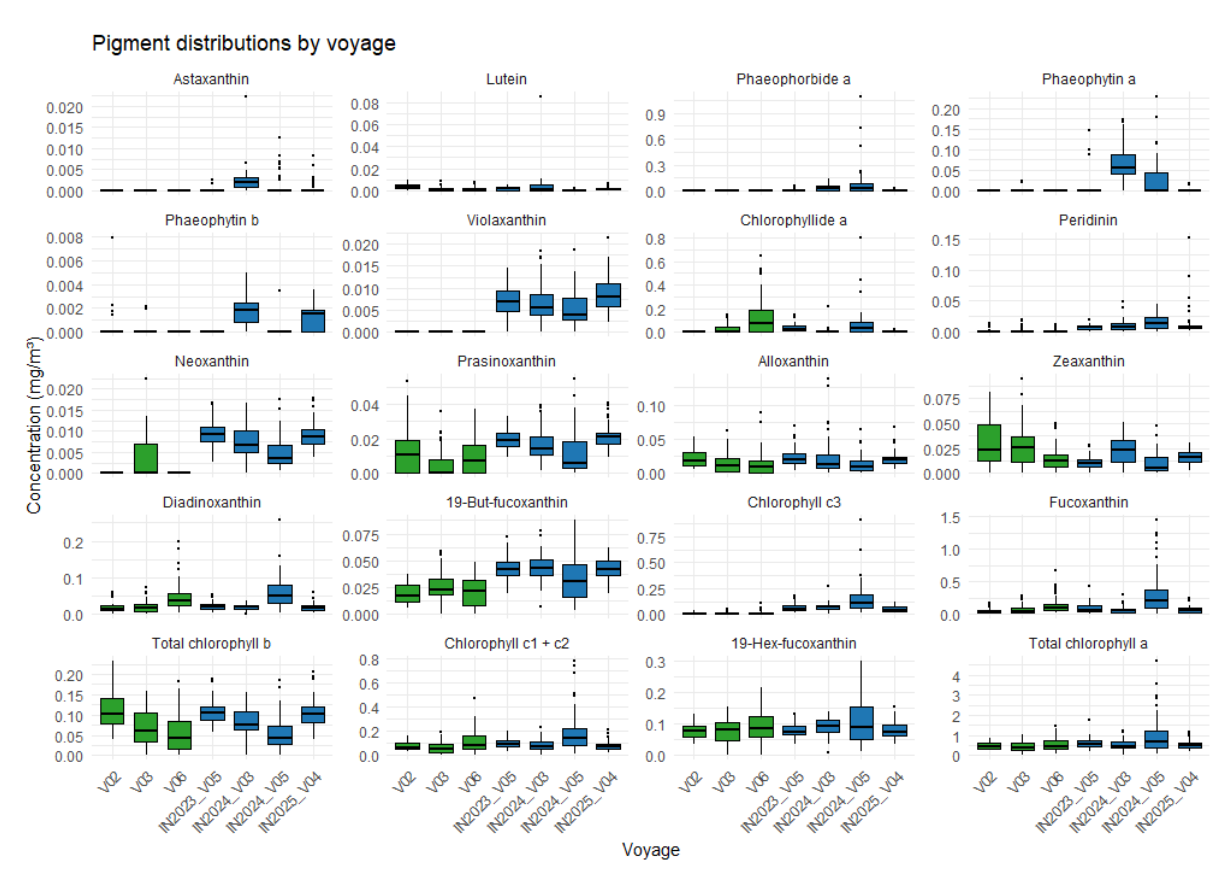


Figure 3 – Pigment concentrations (mg/m⁻³) across SEFES (1990s) and SEAMES (2020s), showing individual voyages.

Ordination analyses

NMDS revealed clear separation of pigment assemblages between SEFES and SEAMES datasets (Fig. 4). Voyage-specific clustering was evident, with SEAMES voyages (IN2023_V05-IN2025_V04) generally grouping toward the lower NMDS1 axis, while SEFES voyages (SS1996 V02-SS1996 V06) occupied the opposite side. This pattern was supported by the pigment significance tests, which showed strong SEAMES-leaning associations for violaxanthin, neoxanthin, but-fucoxanthin, chlorophyll c_3 , peridinin, and various degradation products (p < 0.001), whereas diatoxanthin, zeaxanthin, and chlorophyllide-a were more characteristic of SEFES samples. Voyage ellipses indicated broader spread among voyages SEAMES IN2024 V05, and SEFES voyages SS1996 V03

and SS1996 V06, suggesting greater within-cruise variability in community composition.

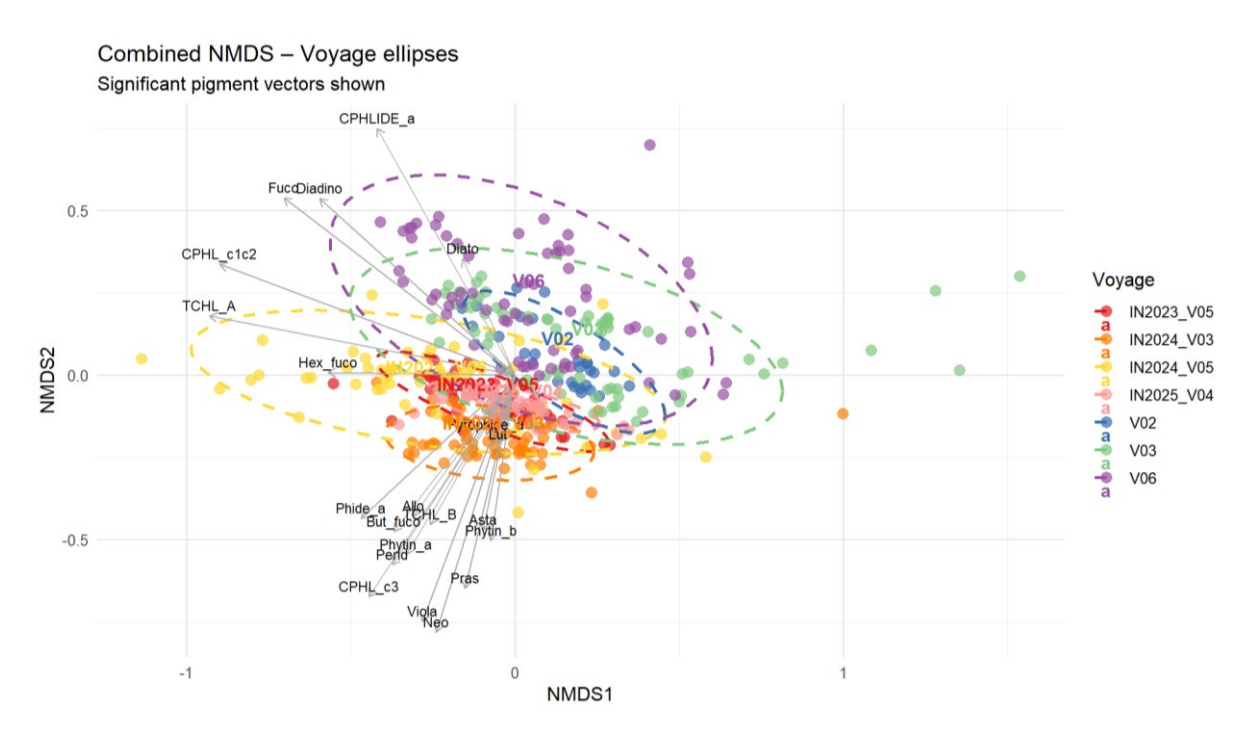


Figure 4 – NMDS ordination of pigment assemblages from SEFES (blue, green, purple) and SEAMES (pink, yellow, orange, red) voyages. Voyage-specific ellipses highlight within-voyage variability, while overlaid pigment vectors indicate the pigments most strongly associated with community structure.

To further examine environmental structuring within each dataset, NMDS ordinations were overlaid with significant pigment vectors and environmental variables (Fig. 5). For SEFES (Fig. 5a), temperature and nitrate were the main correlates of pigment composition, with elevated fucoxanthin, diadinoxanthin, and chlorophyll c aligning with potential localised nitrate enrichment associated with diatom-dominated assemblages. Although nitrate concentrations were generally low during SS1996 V06, elevated values at several stations corresponded with pronounced diatom blooms, likely driven by mesoscale eddy activity and the rapid uptake of newly available nutrients by fast-growing diatoms. Similarly, the SEAMES ordination (Fig. 5b) showed pigment distributions associated with temperature and nitrate, reflecting gradients in mixed-layer nutrient availability across voyages. Higher prasinoxanthin, neoxanthin, and chlorophyll b concentrations under warmer, more stratified conditions indicated greater representation of prasinophytes in the contemporary community.

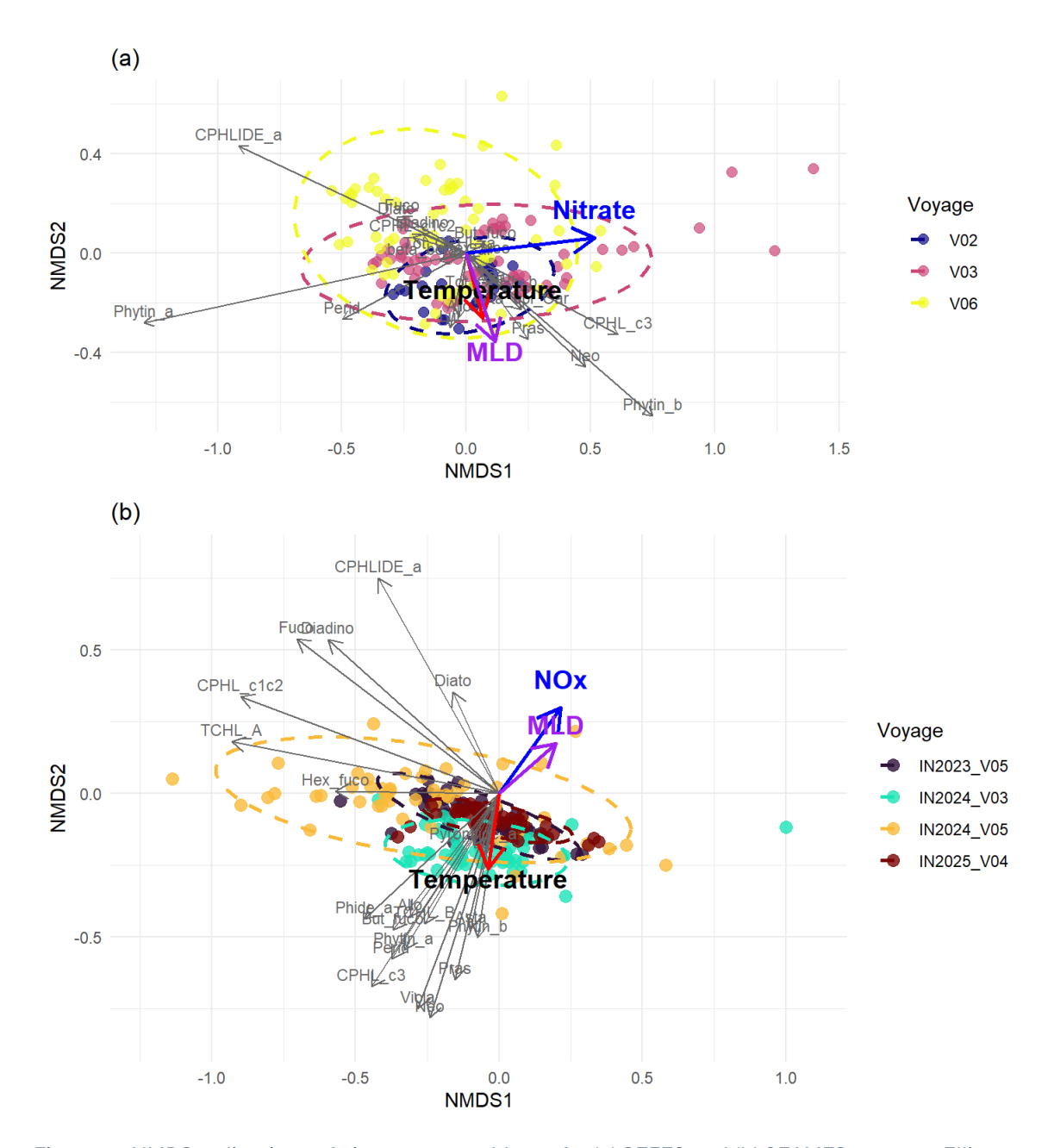


Figure 5 – NMDS ordinations of pigment assemblages for (a) SEFES and (b) SEAMES voyages. Ellipses indicate voyage groupings, with significant pigment (grey), nitrate/NOx (blue), MLD (purple) and temperature (red/black) vectors shown.

Distance-based redundancy analysis (dbRDA) revealed that pigment composition was significantly structured by environmental gradients in both datasets (Fig. 6). For SEAMES, temperature, NOx and MLD were all significant predictors of pigment variability (overall model: F = 4.14, p = 0.001; temperature: F = 6.61, p = 0.002; NOx: F = 3.42, p = 0.002; MLD: F = 2.38, p = 0.022), yet the first two constrained axes together explained only a modest proportion of community variance (adj. $R^2 \approx 2.3\%$). In contrast, the SEFES model showed a stronger relationship between pigment composition and environmental conditions (overall model: F = 5.72, p = 0.001; adj. $R^2 \approx 7.8\%$), with temperature (F = 6.46, p = 0.001), nitrate (F = 7.54, p = 0.001) and MLD (F = 3.18, p = 0.005) all contributing significantly and the first two axes highly

significant (CAP1: F = 9.65, p = 0.001; CAP2: F = 6.12, p = 0.001). The combination of low adjusted R^2 values with strong statistical significance suggests that, while environmental gradients consistently influence pigment assemblages, a large fraction of variance remains unexplained—reflecting either substantial natural spatial-temporal heterogeneity in the system or limitations in sampling coverage—and may be reduced with increased sampling density or targeted process studies.

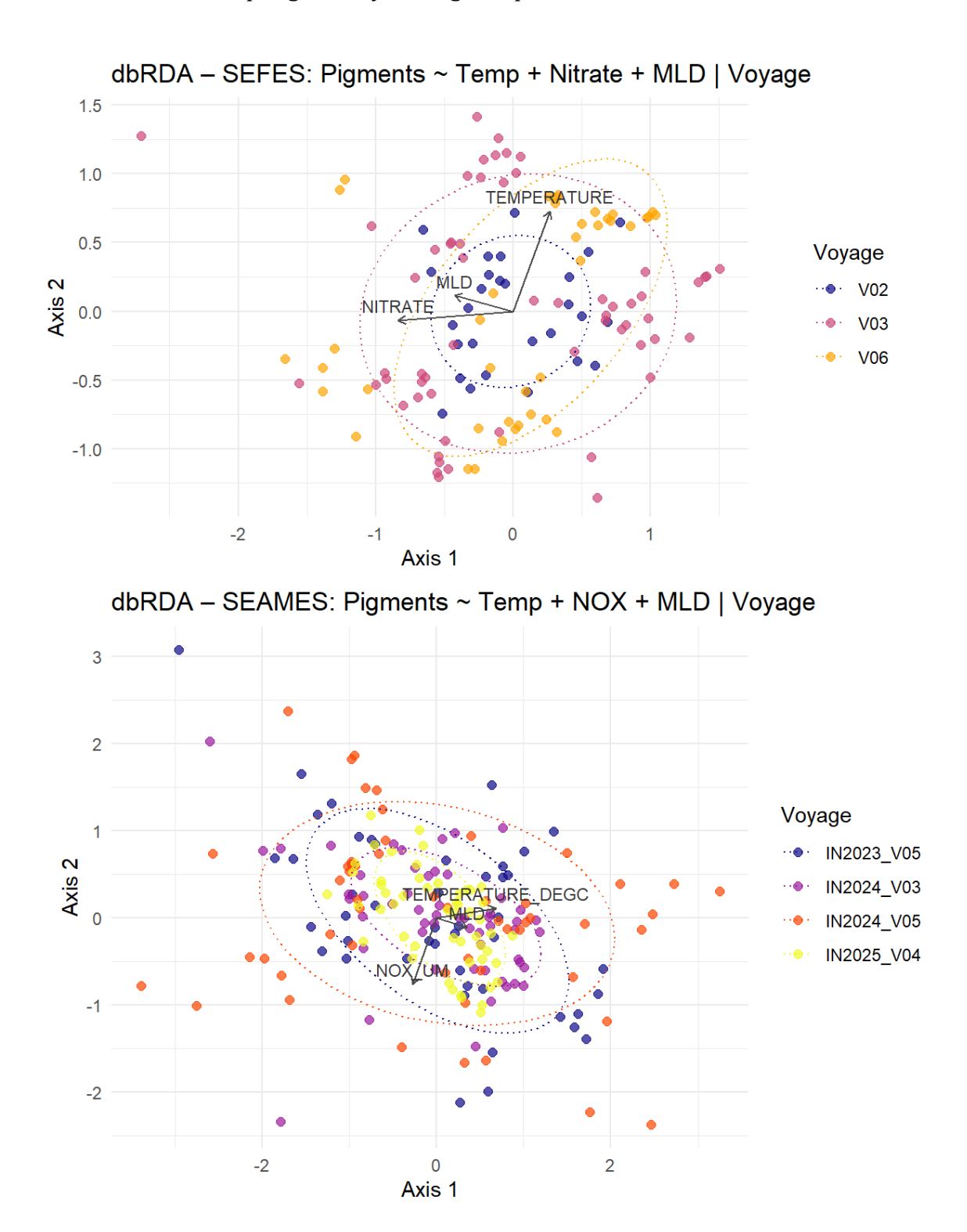


Figure 6 – dbRDA showing the influence of environmental variables on pigment assemblages for SEFES (1990s) and SEAMES (2020s) voyages. Nox/Nitrate, MLD and temperature vectors, factored for Voyage.

Discussion

Across the SEFES (1996) and SEAMES (2023–2025) surveys we demonstrate a temporal reorganisation of phytoplankton communities; recent assemblages carry a stronger imprint of nano- and picoplankton pigments and exhibit a looser, more spatially heterogeneous coupling to physical–nutrient gradients. Temperature, nitrate and MLD remain significant predictors in both eras, but constrained ordinations show these factors explain markedly less pigment variance in SEAMES (adj. $R^2 \approx 2.3\%$) than in SEFES (adj. $R^2 \approx 7.8\%$), consistent with recent forcing producing more patchy and transient ecological states that arise from altered stratification, mixing and mesoscale circulation.

Surface temperature, MLD and nitrate do not act independently but together structure pigment composition. Warm, stratified surface layers were associated with greater representation of prasinophyte and chlorophyte pigments, whereas diatom signals were more closely tied to episodic nutrient delivery and mixing events rather than consistently deeper mixed layers. This covariation appears throughout the violin and NMDS patterns; voyages with similar mean SSTs can differ markedly in nutrient status and pigment distributions, underlining that means obscure distributional complexity (Hallegraeff & Jeffrey, 1993; Winder & Sommer, 2012).

Mechanistically, intensified stratification under a strengthened East Australian Current (EAC) reduces persistent vertical nutrient exchange and shifts the system toward reliance on transient nutrient supply. Under such regimes, small cells with high surface-to-volume ratios are advantaged because they quickly take up small, episodic nutrient inputs (Paerl et al., 2010; Litchman et al., 2015). By contrast, diatoms respond rapidly to larger, short-lived nutrient injections and require turbulence for suspension, which suggests` diatom pigments remain episodically prominent following upwelling or eddy-driven entrainment (Hallegraeff & Reid, 1986; Paerl et al., 2010).

Mesoscale variability in the EAC thus provides the essential context: warm-core eddies suppress nutrient supply and favour small taxa, while cold-core eddies and upwelling events inject slope waters that stimulate diatom growth (Gibbs et al., 1998; Suthers et al., 2011). The autumn SEFES V03 and SEAMES IN2024_V03 cases suggest nuance rather than contradiction: both voyages experienced warm conditions, but their differing nutrient and pigment signatures are consistent with variation in the timing and intensity of mixing and mesoscale forcing, rather than a simple temperature-only response. The 2023–2024 El Niño and strong EAC flow (Geng et al., 2024) during IN2024_V03, for example, coincided with anomalously warm SST, low nitrate and shallow MLD, conditions that corresponded to enhanced prasinophyte type-3 pigments

and likely the success of picoeukaryotes such as *Micromonas* (Meakin & Wyman, 2011; Hoppe et al., 2018).

Comparing decades, dbRDA indicates that environmental control on pigments is statistically consistent but has shifted in strength and spatial coherence; SEFES explained a larger fraction of pigment variance locally, while SEAMES shows significant control but more residual heterogeneity. This pattern is consistent with increased spatial variability in recent physical forcing—stronger EAC fluctuations and episodic eddy activity produce patchy nutrient inputs that increase local heterogeneity in community composition (Schaeffer & Roughan, 2017).

Ecologically, a shift toward nano- and picoplankton dominance implies important changes in trophic pathways and carbon cycling. Smaller cells favour microbial loop pathways and are less likely to form large, rapidly sinking particles, which reduces export efficiency and may lower energy transfer to higher trophic levels (Dickman et al., 2008; Durante et al., 2019). Nonetheless, episodic diatom pulses driven by upwelling or eddy events can still generate short windows of high productivity and quality prey for zooplankton and fish; the net ecosystem effect will therefore depend on the frequency, magnitude and timing of these pulses relative to the prevailing stratified baseline (Oke & Middleton, 2001; Armbrecht et al., 2015).

The study's main limitations derive from inference by proxy and differences in sampling design between decades. Pigments are robust functional markers, but they are indirect indicators of cell size and taxonomic composition; integrating flow cytometry, microscopy and size-fractionated biomass would confirm whether pigment shifts translate to changes in cell abundance, size structure and carbon flux. Spatial heterogeneity and differing cruise strategies likely contribute to residual variance in multivariate models, so targeted process studies that sample eddies and upwelling features synoptically would better resolve the role of episodic drivers.

Looking forward, linking pigment composition with in-situ production rates, particle flux measurements and physical diagnostics of eddy activity will be essential to quantify the biogeochemical consequences of ongoing EAC intensification. Such integration will clarify whether the observed shift toward smaller phytoplankton represents a sustained reorganisation of the shelf ecosystem or reflects a pattern of alternating states driven by episodic nutrient injections. In either case, our results emphasise that changes in temperature and stratification are translated into ecological outcomes through altered nutrient dynamics and mesoscale circulation, with implications for productivity, trophic transfer and carbon export in this rapidly changing boundary-current system.

References

- Armbrecht, L. H., Schaeffer, A., Roughan, M., & Armand, L. K. (2015). Interactions between seasonality and oceanic forcing drive the phytoplankton variability in the tropical-temperate transition zone (~30°S) of Eastern Australia. *Journal of Marine Systems*, *144*, 92-106. https://doi.org/https://doi.org/10.1016/j.jmarsys.2014.11.008
- Bax, N. J., & Williams, A. (2000). *Habitat and fisheries productivity in the south east fishery ecosystem: final report to the Fisheries Research and Development Corporation*. CSIRO Marine Research.
- Behrenfeld, M. J., & Boss, E. (2006). Beam attenuation and chlorophyll concentration as alternative optical indices of phytoplankton biomass. *Journal of marine research*, *64*(3), 431-451. https://doi.org/10.1357/002224006778189563
- Brewin, R. J. W., Sathyendranath, S., Jackson, T., Barlow, R., Brotas, V., Airs, R., & Lamont, T. (2015). Influence of light in the mixed-layer on the parameters of a three-component model of phytoplankton size class. *Remote Sensing of Environment,* 168, 437-450. https://doi.org/10.1016/j.rse.2015.07.004
- Dickman, E. M., Newell, J. M., González, M. J., & Vanni, M. J. (2008). Light, nutrients, and food-chain length constrain planktonic energy transfer efficiency across multiple trophic levels. *Proceedings of the National Academy of Sciences, 105*(47), 18408-18412. https://doi.org/doi:10.1073/pnas.0805566105
- Durante, G., Basset, A., Stanca, E., & Roselli, L. (2019). Allometric scaling and morphological variation in sinking rate of phytoplankton. *Journal of phycology*, *55*(6), 1386-1393. https://doi.org/https://doi.org/10.1111/jpy.12916
- Edgar, G. J., Ward, T. J., & Stuart-Smith, R. D. (2018). Rapid declines across Australian fishery stocks indicate global sustainability targets will not be achieved without an expanded network of 'no-fishing' reserves. *Aquatic Conservation: Marine and Freshwater Ecosystems*, *28*(6), 1337-1350. https://doi.org/https://doi.org/10.1002/aqc.2934
- Everett, J. D., Baird, M. E., Oke, P. R., & Suthers, I. M. (2012). An avenue of eddies: Quantifying the biophysical properties of mesoscale eddies in the Tasman Sea. *Geophysical Research Letters*, *39*(16). https://doi.org/https://doi.org/10.1029/2012GL053091
- Falkowski, P. (2012). Ocean Science: The power of plankton. *Nature (London)*, *483*(7387), S17-S20. https://doi.org/10.1038/483S17a
- Geng, X., Kug, J.-S., Shin, N.-Y., Zhang, W., & Chen, H.-C. (2024). On the spatial double peak of the 2023–2024 El Niño event. *Communications Earth & Environment*, *5*(1), 691. https://doi.org/10.1038/s43247-024-01870-1
- Gibbs, M. T., Middleton, J. H., & Marchesiello, P. (1998). Baroclinic Response of Sydney Shelf Waters to Local Wind and Deep Ocean Forcing. *Journal of Physical Oceanography*, *28*(2), 178-190. https://doi.org/https://doi.org/10.1175/1520-0485(1998)028<0178:BROSSW>2.0.CO;2
- Hallegraeff, G., & Jeffrey, S. (1993). Annually recurrent diatom blooms in spring along the New South Wales coast of Australia. *Marine and Freshwater Research*, *44*(2), 325-334. https://doi.org/https://doi.org/10.1071/MF9930325
- Hallegraeff, G., & Reid, D. (1986). Phytoplankton species successions and their hydrological environment at a coastal station off Sydney. *Marine and Freshwater Research*, *37*(3), 361-377. https://doi.org/https://doi.org/10.1071/MF9860361

- Hooker, S., Clementson, L., Thomas, C., Schlüter, L., Allerup, M., & Ras, J. (2012). The Fifth SeaWiFS HPLC Analysis Round-Robin Experiment (SeaHARRE-5) Rep. *Greenbelt, MA, NASA Goddard Space Flight Center,* 1-108.
- Hoppe, C. J. M., Flintrop, C. M., & Rost, B. (2018). The Arctic picoeukaryote Micromonas pusilla benefits synergistically from warming and ocean acidification. *Biogeosciences*, *15*(14), 4353-4365. https://doi.org/10.5194/bg-15-4353-2018
- Jeffrey, S. W. (1974). Profiles of photosynthetic pigments in the ocean using thin-layer chromatography. *Marine Biology*, *26*(2), 101-110. https://doi.org/10.1007/BF00388879
- Litchman, E., de Tezanos Pinto, P., Edwards, K. F., Klausmeier, C. A., Kremer, C. T., & Thomas, M. K. (2015). Global biogeochemical impacts of phytoplankton: a trait-based perspective. *Journal of Ecology*, *103*(6), 1384-1396. https://doi.org/https://doi.org/10.1111/1365-2745.12438
- Meakin, N. G., & Wyman, M. (2011). Rapid shifts in picoeukaryote community structure in response to ocean acidification. *The ISME Journal*, *5*(9), 1397-1405. https://doi.org/10.1038/ismej.2011.18
- Oke, P. R., & Middleton, J. H. (2001). Nutrient enrichment off Port Stephens: the role of the East Australian Current. *Continental Shelf Research*, *21*(6), 587-606. https://doi.org/https://doi.org/10.1016/S0278-4343(00)00127-8
- Paerl, H. W., Rossignol, K. L., Hall, S. N., Peierls, B. L., & Wetz, M. S. (2010). Phytoplankton Community Indicators of Short- and Long-term Ecological Change in the Anthropogenically and Climatically Impacted Neuse River Estuary, North Carolina, USA. *Estuaries and Coasts*, *33*(2), 485-497. https://doi.org/10.1007/s12237-009-9137-0
- Poloczanska, E. S., Brown, C. J., Sydeman, W. J., Kiessling, W., Schoeman, D. S., Moore, P. J., Brander, K., Bruno, J. F., Buckley, L. B., Burrows, M. T., Duarte, C. M., Halpern, B. S., Holding, J., Kappel, C. V., O'Connor, M. I., Pandolfi, J. M., Parmesan, C., Schwing, F., Thompson, S. A., & Richardson, A. J. (2013). Global imprint of climate change on marine life. *Nature Climate Change*, *3*(10), 919-925. https://doi.org/10.1038/nclimate1958
- Ridgway, K. R., & Ling, S. D. (2023). Three decades of variability and warming of nearshore waters around Tasmania. *Progress in Oceanography, 215*, 103046. https://doi.org/https://doi.org/10.1016/j.pocean.2023.103046
- Schaeffer, A., & Roughan, M. (2017). Subsurface intensification of marine heatwaves off southeastern Australia: The role of stratification and local winds. *Geophysical Research Letters*, *44*(10), 5025-5033. https://doi.org/https://doi.org/10.1002/2017GL073714
- Suthers, I. M., Young, J. W., Baird, M. E., Roughan, M., Everett, J. D., Brassington, G. B., Byrne, M., Condie, S. A., Hartog, J. R., Hassler, C. S., Hobday, A. J., Holbrook, N. J., Malcolm, H. A., Oke, P. R., Thompson, P. A., & Ridgway, K. (2011). The strengthening East Australian Current, its eddies and biological effects an introduction and overview. *Deep Sea Research Part II: Topical Studies in Oceanography*, *58*(5), 538-546. https://doi.org/https://doi.org/10.1016/j.dsr2.2010.09.029
- Uitz, J., Claustre, H., Morel, A., & Hooker, S. B. (2006). Vertical distribution of phytoplankton communities in open ocean: An assessment based on surface chlorophyll. *Journal of Geophysical Research. C. Oceans, 111*(C8), C08005--n/a. https://doi.org/10.1029/2005JC003207

Winder, M., & Sommer, U. (2012). Phytoplankton response to a changing climate. *Hydrobiologia*, 698(1), 5-16. https://doi.org/10.1007/s10750-012-1149-2
Zhou, X., Li, D., Jing, Z., Wu, L., Cai, W., Li, Z., & Shi, J. (2025). Eddies Redistribute Ocean Warming Hotspots in the East Australian Current Southern Extension. *Geophysical Research Letters*, 52(16), e2025GL116772. https://doi.org/https://doi.org/10.1029/2025GL116772

Acknowledgements

JCG thanks Claire Davies and Albertina Dias for their invaluable contributions, conversations and guidance. Thanks also extended to Prof. Zanna Chase for facilitating and guiding this research project.

Data availability

All raw data supplied by CSIRO. Code used to generate outputs shared with CSIRO.

Appendix

Table S1 – Significant pigments across voyage groups. Positive statistic values are "SEAMES leaning" while negative values are "SEFES leaning".

pigment	group1	group2	statistic	df	signif	p_plain	p_adj_plain
viola	seames	sefes	25.3267954	215.0000	***	0.000	0.000
neo	seames	sefes	16.4552180	354.3117	***	0.000	0.000
but_fuco	seames	sefes	13.0138569	365.8377	***	0.000	0.000
chl_c3	seames	sefes	12.1011293	238.9383	***	0.000	0.000
perid	seames	sefes	10.2713259	245.6369	***	0.000	0.000
phytin_a	seames	sefes	8.9551868	216.8550	***	0.000	0.000
pras	seames	sefes	8.6655502	328.6744	****	0.000	0.000
phytin_b	seames	sefes	7.5968300	365.8298	****	0.000	0.000
asta	seames	sefes	7.0070335	215.0000	****	0.000	0.000
pyro_phide_a	seames	sefes	5.5797529	215.0000	****	0.000	0.000
phide_a	seames	sefes	4.9200813	215.0000	****	0.000	0.000
diato	seames	sefes	-4.8910675	183.3411	****	0.000	0.000
zea	seames	sefes	-4.6024228	233.8388	****	0.000	0.000
tchl_a	seames	sefes	4.1706654	337.0252	****	0.000	0.000
tchl_b	seames	sefes	3.3453529	300.1627	**	0.001	0.001
chlide_a	seames	sefes	-3.2456933	251.5474	**	0.001	0.002
allo	seames	sefes	2.9623638	367.4587	**	0.003	0.004
fuco	seames	sefes	2.4171554	337.5642	*	0.016	0.019
hex_fuco	seames	sefes	1.6241276	355.7662	ns	0.105	0.116

pigment	group1	group2	statistic	df	signif	p_plain	p_adj_plain
lut	seames	sefes	0.4596213	294.0229	ns	0.646	0.678
diadino	seames	sefes	-0.1535868	338.5840	ns	0.878	0.878